

Band offsets measured by internal photoemission-induced second-harmonic generation

Z. Marka, R. Pasternak, S. N. Rashkeev, Y. Jiang, S. T. Pantelides, and N. H. Tolk
Department of Physics and Astronomy, Vanderbilt University, Nashville, Tennessee 37235

P. K. Roy
Agere Systems, Orlando, Florida 32819

J. Kozub
Free-Electron Laser Center, Vanderbilt University, Nashville, Tennessee 37235
 (Received 15 August 2002; published 6 January 2003)

We report first band-offset measurements obtained by multiphoton internal-photoemission induced second-harmonic generation. Our two-color contactless laser technique involves (1) optically pumping electrons into the oxide and (2) probing the resulting interface electric field using time-dependent second-harmonic generation. One- and two-photon internal-photoemission thresholds for the Si/SiO₂ interface were measured to be 4.5 and 2.25 eV, respectively. This method promises to become a valuable experimental tool in determining band offsets in wide variety of semiconductor interfaces.

DOI: 10.1103/PhysRevB.67.045302

PACS number(s): 73.50.Gr, 73.40.-c, 42.65.Ky, 77.55.+f

The past few decades have seen a rapid increase in component density in integrated circuits. The resulting decrease in channel lengths in MOSFET's requires gate oxide thicknesses to be scaled down to 4 nm and below. As a result, new physics issues arise involving enhanced electron tunneling through ultrathin oxide films. Because of inherent limitations in ultrathin SiO₂, some high-*k* dielectric materials have been investigated as a replacement for silicon dioxide. Carrier transport across interfaces and charge trapping in gate oxides are essential factors in defining device performance and degradation. In the first approximation the main determining factor in charge injection processes is the band structure of the semiconductor/oxide interface. Knowledge of conduction and valence band offsets is crucial in determining whether electron or hole injection is possible under certain excitations. For many new alternative and chemically modified oxides under investigation these band offsets are not well characterized, both theoretically and experimentally.

Electric field induced second-harmonic (EFISH) generation has attracted particular attention during the past few years as an effective method for interface studies.^{1,2} The second-harmonic signal is not only sensitive to applied static fields but also to quasistatic electric fields resulting from charge separation created by carrier injection processes. It was shown first by van Driel and collaborators³ and confirmed by others,^{4,5} that for thin SiO₂ on silicon (below 10 nm) a time-dependent second-harmonic generation (SHG) signal may be readily observed. The time-dependent SHG signal is due to the interface electric field created by the injected and subsequently surface-trapped electrons. The high electron affinity of the ambient surface oxygen plays a key role in the formation of the surface trap states. The time dependence of the SHG signal provides an information about the electron injection, transport, and trapping processes.

Second-harmonic generation has been proven to be a novel, nondestructive probe technique for Si/oxide interfaces. It has been used to study surface charge trapping processes in the presence of different ambient gases.⁶ It has been applied to the characterization of x-ray irradiation induced

oxide traps in SiO₂,⁵ and electron and hole injection processes at the Si/(ZrO₂)_x(SiO₂)_{1-x} interface.⁷ These experiments were all based on detecting the time-dependent SH signal originating from the quasistatic interface electric field created by charge injection and trapping.

Most of the previous time-dependent EFISH experiments have been performed using a single laser source, primarily the Ti:sapphire laser, operating in the wavelength range, 720–900 nm. In this case the incident laser beam is used for two purposes. First, it creates electron-hole pairs via a single or multiphoton process, which if energetically feasible, allows the injection of electrons into the oxide. Second, the interfacial electric field, that arises from charge separation caused by injection and trapping, may then be detected by the SHG signal generated by the same laser beam. By using a mercury arc lamp in addition to a Ti:sapphire laser, van Driel and co-workers have shown that the electron injection process can be enhanced by an additional pumping source.³ In our experiments, we employ two separate tunable laser sources. The first laser operating in the visible and UV serves to optically pump electrons into the oxide and the second laser operating in the near IR probes the resulting interface electric field using the time-dependent second-harmonic generation technique. Thus, the pump and probe functions are separated.

In this paper we apply a two-color technique involving time-dependent EFISH combined with an additional widely tunable laser source for carrier injection, as a sensitive method for determining band offsets at semiconductor interfaces. We suggest that wavelength dependent measurements can identify and measure thresholds in multiphoton carrier injection processes from which the energy difference between a semiconductor valence and an oxide conduction band (for electron injection) or a semiconductor conduction and an oxide valence band (for hole injection) may be obtained. First, we have applied these concepts to the well-known Si/SiO₂ interface.

In order to compare electron injection and trapping rates for different laser powers and for different light wavelengths,

we used a high intensity tunable visible/UV laser for injecting electrons into the oxide and used an IR laser beam operating at a lower intensity and at a constant wavelength to monitor the time-dependent electric field via SHG.⁸ The injection (or pump) laser source was a widely tunable (1–6 eV), high pulse power ($>5 \mu\text{J}/\text{pulse}$), 1 kHz repetition rate OPG (optical parametric generator). We used a Ti:sapphire laser with a 76 MHz repetition rate at 800 nm as an SHG probe laser. The probe laser beam was incident on the sample at a 45° angle, and we detected the second-harmonic in a $p(\text{in})/p(\text{out})$ configuration. We used the 800 nm probe beam at fairly low peak intensity ($3.3 \text{ GW}/\text{cm}^2$) and also decreased its duty factor by a factor of 16 (using a shutter) so that this beam gives a minimal contribution to the charge carrier injection process. All data presented here were taken under identical probe laser beam conditions. The pump beam was diverted to the sample at close to normal incidence, and we took data at several peak intensities for each pump laser wavelength. We also made sure that we did not reach the damage threshold of Si throughout the studied wavelength range. The pump laser spot size diameter in our experiments varied in the range $\sim 100\text{--}300 \mu\text{m}$ depending on the wavelength used. In general, for higher order injection processes we used smaller spot sizes to obtain higher peak intensities. We used a focusing lens to vary the spot size, and at each wavelength we put neutral density filters into the beam path in order to vary the intensity of the incident radiation. The power fluctuation of the injection laser was also monitored continuously via diverting a small portion of the beam into a pyroelectric meter, which was calibrated against a pulse energy meter.

The sample used was a conventional, thermally grown 42 Å thick SiO_2 deposited on Si(100) provided by Lucent Technologies. At this oxide thickness, the injected electrons reach the surface with a high probability, giving rise to a large field and, therefore, to a large, easily detectable time-dependent SHG signal.⁶ This oxide is also thick enough to neglect the electron tunneling from the surface back to the interface.⁹ Figure 1(a) shows a typical example of a time-dependent pump-probe type SHG measurement performed for our 42 Å thick Si/SiO₂ sample. When the injection beam was turned on, the signal rose rapidly indicating the creation of a time-dependent quasistatic electric field. This field originates from charge separation across the interface due to trapping of injected electrons at the oxide surface by the ambient oxygen, while the holes remain in Si. After a steady-state signal was reached, we blocked the injection beam and observed that the signal does not change anymore. This is in a contrast with our observations on a 17 Å sample [Fig. 1(b)]. For this ultrathin sample case, when we blocked the pump beam, the SHG signal was observed to slowly decrease in intensity indicating an increasingly lessened electric field across the interface. A similar behavior was observed for oxide thicknesses below a critical value ($\sim 30 \text{ \AA}$), for which electron tunneling rates are significant. In such a case, a detrapping from the O₂-rich surface and subsequent recombination with holes at the interface occur within a short time.

Figure 2 shows the time-dependent SHG signal measured for several different pump beam intensities. The pump wave-

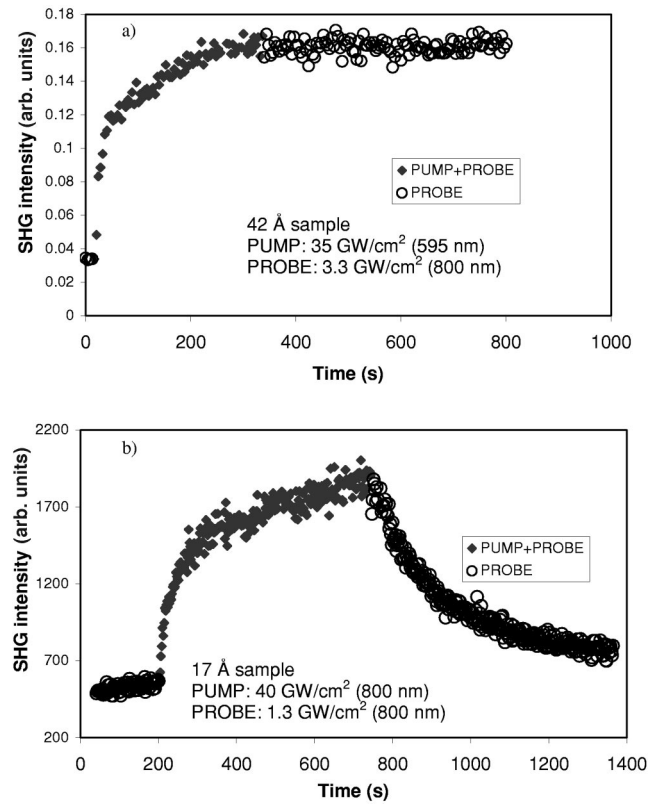


FIG. 1. (a) Pump-probe type time-dependent SHG data for a 42 Å thick oxide sample compared to (b), the same for a 17 Å sample. After the pump laser is turned off, the SHG signal decreases for the thinner sample, indicating that electrons tunnel back to the interface.

length was 516 nm (2.4 eV). As the injection beam intensity increases, the SH signal reaches the saturation level at an earlier time indicating an enhancement in the injection rate. The experiments discussed here were performed using ultrafast high intensity pulsed laser sources. Pump-probe experiments, where the time delay between pump and probe pulses was varied, performed on Si/SiO₂ structures by Dadap *et al.*,¹⁰ showed a transient increase in the SHG intensity during the laser pulse. They attributed this effect to screening. The gradual increase in the SHG signal, and, therefore, in the electric field, observed in our experiment (Fig. 2) is due to a small number of excited electrons which are injected into the oxide, transported through the oxide and trapped at the surface. After each consecutive laser pulse, the density of electrons trapped at the oxide surface increases cumulatively, until a steady-state level is reached, determined by the density of available trap sites, oxide thickness dependent transport, and band bending.

The time-dependent SHG from the Si/SiO₂ interface can be described in general by

$$I^{2\omega}(t) = |\chi^{(2)} + \chi^{(3)}E(t)|^2 (I^\omega)^2, \quad (1)$$

where I^ω and $I^{2\omega}(t)$ are the intensities of the fundamental beam and the TDSHG signal, $\chi^{(2)}$ is the effective second-order susceptibility from all other sources, $\chi^{(3)}$ is the third-order nonlinear susceptibility of Si nearby the interface, and

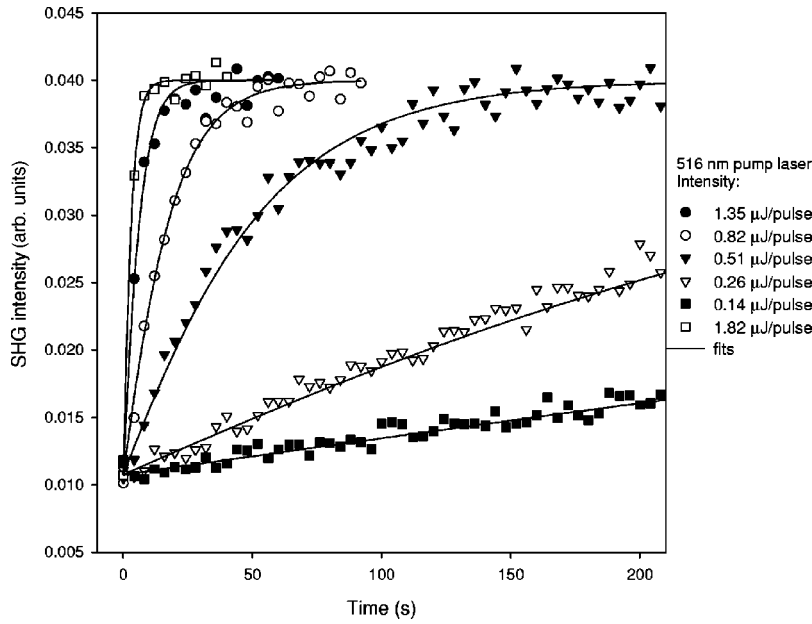


FIG. 2. Time-dependent electric field induced SHG signals for varying pump intensities at the 516 nm wavelength. The black lines show the fits to the data using Eq. (4).

$E(t)$ is a quasistatic electric field in the silicon space charge region at the Si/SiO₂ interface. $E(t)$ arises from the charge separation at the interface and is localized within a thin Si/SiO₂ interface region,¹¹ which is much thinner than the coherence length for the SHG signal. Therefore, the interference and the internal homodyne effect which may be important when the susceptibility $\chi^{(3)}$ comes mainly from the bulk of the sample,^{2,12} do not significantly contribute in our present case and cannot affect our results and their interpretation.

The time dependent electric field is a measure of the electron density accumulated at the oxide surface. We were able to reasonably fit our data to the model that suggests the presence of the only one type of traps in the system (i.e., the surface traps). Other types of traps in the bulk of the oxide or at the interface may also exist. However, it is reasonable to assume that the densities of these traps (e.g., interface traps) are low and that they can be filled up in a very short time. Separate experiments performed by our group on x-ray irradiated Si/SiO₂ samples did show that new trap centers, besides the surface electron traps, could be formed due to radiation damage.⁸

In Eq. (1) the quasistatic electric field is proportional to the density of the charged electron traps at the surface, which can be given through the solution of the rate equation

$$\frac{dn_e}{dt} = (n_{0e} - n_e)/\tau_{\text{pump}}^e + (n_{0e} - n_e)/\tau_{\text{probe}}^e - n_e/\tau_{\text{detrapp}}^e, \quad (2)$$

where n_{0e} describes the initial number of unfilled electronic traps, $1/\tau_{\text{pump}}^e$ and $1/\tau_{\text{probe}}^e$ give the rates of filling up the surface electronic trap states due to the pump and probe beams (the second one is usually negligible in comparison with the first one). τ_{detrapp}^e characterizes the lifetime of the electron trap states at the surface. It contains contributions from the rate describing the detrapping of surface electrons, the tunneling rate for electrons through the oxide, and their

recombination rate (with holes) at the interface. We found that τ_{detrapp}^e is of the order of several hours for a ~ 40 Å thick oxide. This is much longer than a typical time scale of one measurement in our experimental setup.

Since the rate $1/\tau_{\text{pump}}^e$ is significantly higher than the other two rate constants in Eq.(2), the solution can be easily found:

$$n_e(t) = n_{0e} \cdot (1 - e^{-t/\tau_{\text{pump}}^e}). \quad (3)$$

Therefore, our time-dependent EFISH data can be fitted by a formula

$$I^{2\omega}(t) = |y_0 + a \cdot (1 - e^{-t/\tau_{\text{pump}}^e})|^2, \quad (4)$$

where y_0 and a are phenomenological values related to the initial and saturation SHG levels. We have determined the parameter $1/\tau_{\text{pump}}^e$ for a large range of incident pump beam intensities at several different wavelengths between 258 and 663 nm. When fitting our data we did not take into account the relative phase between the two susceptibility components, or between the $\chi^{(2)}$ and $\chi^{(3)}$ terms, in Eq. (1) [or between the y_0 and a terms in Eq. (4)]. We studied how a relative phase affects the fitted rate constants and found that our intensity dependent data could be fitted adequately if the phase shift is not higher than 45° .¹³ This uncertainty introduces a less than 7% error to the value of the fitted parameter $1/\tau_{\text{pump}}^e$. This is not very important since the purpose of the present investigation is to compare rates at several different wavelengths and not to find their exact value.

Figure 3 shows the dependence of the $1/\tau_{\text{pump}}^e$ rate constants on the pump laser intensity at the 516 nm wavelength. Fitting these intensity dependent data to $1/\tau_{\text{pump}}^e \propto (I_{\text{pump}})^n$ gives a slope of 2.26 ± 0.10 , which we associate with the number of photons required in the injection process at 516 nm (2.4 eV). Here we assumed that the measured trap-filling rate $1/\tau_{\text{pump}}^e$ is proportional to the probability of the n -photon interband transition given by

$$W_n = K_n (I^\omega)^n / (n\hbar\omega), \quad (5)$$

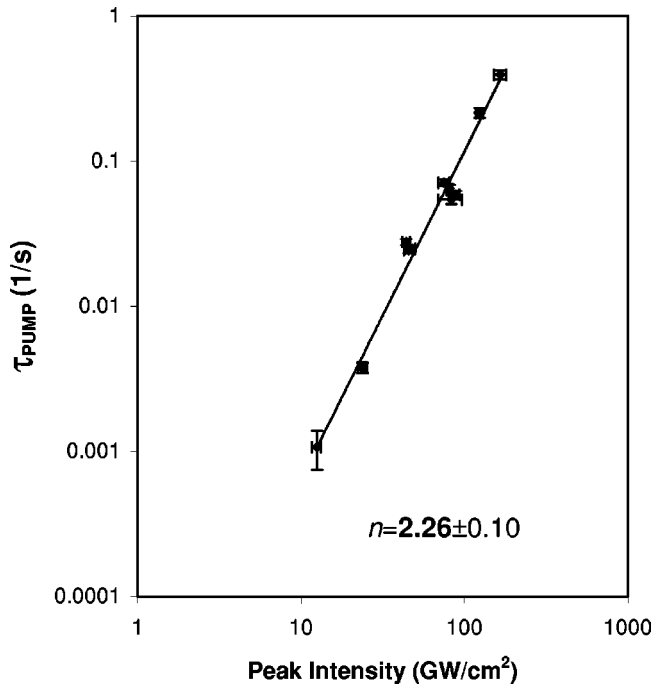


FIG. 3. Electron trap-filling rate constants versus pump laser (516 nm) intensity, determined by fitting the time-dependent EFISH data. The solid line is the best fit based on a simple power law. It indicates an approximately quadratic dependence of the rate on the laser intensity.

where K_n is the n -photon absorption coefficient, I^ω is the incident beam intensity at the energy $\hbar\omega$.¹⁴

The number of photons required to inject electrons from silicon to SiO_2 was determined for several different energies in the 1.9–4.8 eV incident pump energy range [Fig. 4(a)]. As illustrated in Fig. 3 for a particular pump wavelength of 516 nm, the multiphoton numbers, n , describing the order of the injection process for each wavelength were deduced from the dependence of the measured trap-filling rate constants $1/\tau_{\text{pump}}^e$ on the pump laser intensity. The main features that appear in Fig. 4(a) are the stepwise jumps from one- to two-photon (between 4.56 and 4.50 eV) and then from two- to three-photon (between 2.30 and 2.20 eV) processes as the incident pump energy decreases. To the best of our knowledge, this is the first time when multiphoton internal photoemission thresholds were observed. The energies, where the stepwise jumps are observed, are identified with the thresholds for the one-photon (~ 4.53 eV) and two-photon (~ 2.25 eV) electron injection from Si valence band (VB) into the SiO_2 conduction band (CB).

Published values for the Si(VB)- SiO_2 (CB) offset generally vary in the 4.05–4.6 eV range.^{15,16} The wide variation is usually attributed to the presence of excitonic levels in the SiO_2 band gap. Measured thresholds in internal photoemission (IPE) studies¹⁷ are in the range of 4.05–4.35 eV,¹⁵ where the lowest value is attributed to mobile ion contamination in the oxide. IPE measurements are generally performed on MOS structures, where the oxide thickness is of the order of 1 μm . In a recent study, Afanas'ev et al found that the Si(100)(VB)- SiO_2 (CB) barrier of 4.25 eV is un-

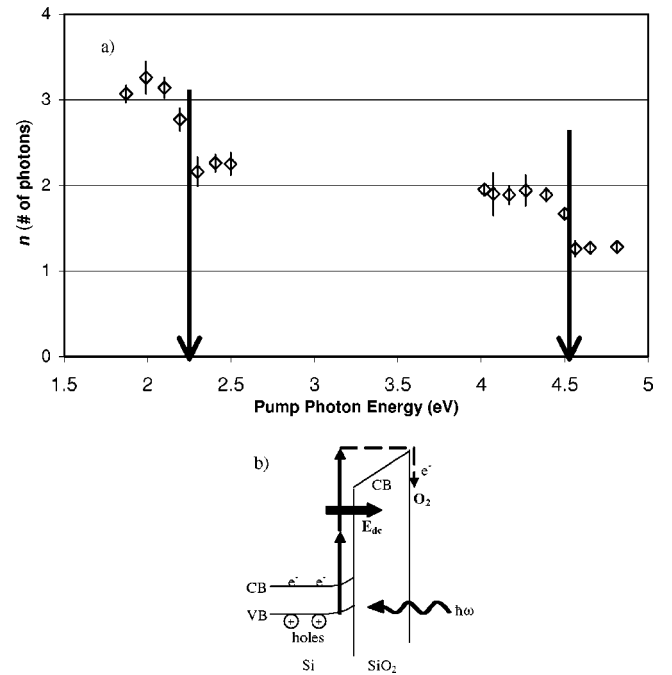


FIG. 4. (a) The order of electron injection process from silicon into SiO_2 versus the photon energy of the pump beam, determined from the intensity dependence of injection rates, (b) schematic representation of electron injection and transport process in the Si/ SiO_2 system.

changed down to oxide thicknesses of ~ 10 Å (IPE).¹⁸ A recent experimental study by the Lucovsky's group determined 4.35 eV for the Si(100)(VB)- SiO_2 (VB) offset via x-ray photoemission method.¹⁹ This gives 4.6 eV for Si(VB)- SiO_2 (CB) difference if one uses 8.95 eV (Ref. 20) for the SiO_2 bandgap.

Our experimental result of ~ 4.5 eV for the electron injection threshold in the Si/ SiO_2 system is in a good agreement with the data cited above. For the interpretation of this result, it is important to mention that with our methodology we do not necessarily measure the barrier between the “flat” Si valence and SiO_2 conduction bands. We deduce the order of the internal photoemission process from the measured electron trap filling rates up to a saturation level. This means that there may be a significant band bending due to the electric field created by the trapped electrons at the oxide surface. This effect increases the barrier height to injection. The maximal increase in the measured offset due to band bending is given by

$$eE_{\text{dc}}d_{\text{oxide}} = (e^2 n_e^\infty d_{\text{oxide}}) / \epsilon_{\text{Si}}, \quad (6)$$

where e is the electron charge, d_{oxide} is the thickness of the SiO_2 layer (42 Å), n_e^∞ is the surface charge density at the time $t = \infty$, and ϵ_{Si} is the dielectric constant of Si. The surface charge density can be estimated by comparing the results of our EFISH measurements with the data available on dc-biased MOS samples,²¹ and also with the data on thickness dependence of the time-dependent EFISH process.²² We estimate the steady-state charge density of the surface-trapped electrons to be around $n_e^\infty \sim 3 \times 10^{12} \text{ cm}^{-2}$,¹³

which results in a 0.19 eV maximum increase in barrier height due to band bending. Additionally, the injected electrons also need to overcome the activation energy for electron hopping (0.1 eV),²³ which is required for the electron to move away from the interface.

Figure 4(a) shows, that the two-photon injection threshold obtained by our technique is not less precise than the one-photon threshold. This suggests that the band structure information obtained from thresholds observed for higher order processes, for which the selection rules are different,¹⁴ can complement results obtained from linear optical measurements. Additionally, since high-intensity ultrafast laser sources are now widely available, the experimental work is no longer limited to threshold studies in the linear absorption regime. Also, we do not expect that the multiphoton excitonic absorption will affect the value of the observed threshold. While conventional IPE measurements are performed on semiconductor/insulator interfaces with a metallic contact, our methodology involving SHG is a contactless technique, which probes exclusively the interface band structure in question. It is always hard to produce good quality contacts on ultrathin oxides, and this fact makes conventional IPE studies on ultrathin samples less reliable. Our two-color methodology utilizes EFISH for probing the interface. This technique relies on measuring the time-dependent changes of the interface fields due to the charge trapping in the bulk or at the surface of the oxide. It is especially advantageous for thin oxide (<100 Å) studies, where the EFISH signal is greatly enhanced by surface electron trapping processes.

In summary, we have made first measurements of the Si valence to SiO₂ conduction band offset via multiphoton internal-photoemission induced second-harmonic generation. Our two-color nondestructive laser technique involves a two-step process. First, electrons are excited by a tunable pump laser (in a single- or multiple-photon process) into the conduction band of silicon. Depending on the excitation energy, the electrons may then be injected into the oxide and get trapped at the oxide surface. Second, the interface electric field resulting from the carrier separation is probed using a time-dependent second-harmonic generation technique. We found that the one- and two-photon thresholds for electron injection in the Si/SiO₂ system are ~ 4.5 and ~ 2.25 eV, respectively, what is in a good agreement with the published band offset values for the Si/SiO₂ system. This means that the multiphoton internal-photoemission induced second-harmonic generation technique developed here is a promising experimental tool in determining band offsets in a wide variety of semiconductor interfaces including unconventional and chemically modified oxides. This contactless technique can be easily applied to many crystalline and amorphous materials and to their interfaces. An additional advantage of time-dependent EFISH measurements is that it readily provides dynamical information about the carrier injection, tunneling, and trapping rates.

We gratefully acknowledge funding and support from ONR under Grants Nos. N00014-94-1-1023, N00014-94-1-0995, and N00014-96-1-1286, and AFOSR Grant F-49620-99-1-0289. We also acknowledge valuable discussions with L. C. Feldman.

¹G. Lupke, Surf. Sci. Rep. **35**, 75 (1999).

²O. A. Aktsipetrov, A. A. Fedyanin, A. V. Melnikov, E. D. Mishina, A. N. Rubtsov, M. H. Anderson, P. T. Wilson, M. ter Beek, X. F. Hu, J. I. Dadap, and M. C. Downer, Phys. Rev. B **60**, 8924 (1999).

³J. G. Mihaychuk, J. Bloch, Y. Liu, and H. M. van Driel, Opt. Lett. **20**, 2063 (1995); J. Bloch, J. G. Mihaychuk, and H. M. van Driel, Phys. Rev. Lett. **77**, 920 (1996).

⁴M. Cernusca, R. Heer, and G. A. Reider, Appl. Phys. B: Lasers Opt. **66**, 367 (1998); S. T. Cundiff and T. M. Fortier, Proc. SPIE **3944**, 646 (2000); V. Formenko, C. Hurth, T. Ye, and E. Borguet, J. Appl. Phys. **91**, 1 (2002).

⁵Z. Marka *et al.*, IEEE Trans. Nucl. Sci. **47**, 2256 (2000).

⁶N. Sahmir, J. G. Mihaychuk, H. M. van Driel, and H. J. Kreuzer, Phys. Rev. Lett. **82**, 359 (1999).

⁷Yu. D. Glinka, W. Wang, S. K. Singh, Z. Marka, S. N. Rashkeev, Y. Shirokaya, R. Albridge, S. T. Pantelides, N. H. Tolk, and G. Lucovsky, Phys. Rev. B **65**, 193103 (2002).

⁸A detailed description of the experimental setup can be found in Z. Marka, R. Pasternak, R. G. Albridge, S. N. Rashkeev, S. T. Pantelides, N. H. Tolk, B. K. Choi, D. M. Fleetwood and R. D. Schrimpf, J. Appl. Phys. (to be published).

⁹M. L. Green, E. P. Gusev, R. Degraeve, and E. L. Garfunkel, J. Appl. Phys. **90**, 2057 (2001).

¹⁰J. I. Dadap, P. T. Wilson, H. M. Anderson, and M. C. Downer,

Opt. Lett. **22**, 901 (1997).

¹¹W. Wang, G. Lupke, M. Di Ventra, S. T. Pantelides, J. M. Gilligan, N. H. Tolk, I. C. Kizilyalli, P. K. Roy, G. Margaritondo, and G. Lucovsky, Phys. Rev. Lett. **81**, 4224 (1998).

¹²T. V. Murzina, A. A. Fedyanin, T. V. Misuryaev, G. B. Khomutov, and O. A. Aktsipetrov, Appl. Phys. B: Lasers Opt. **68**, 537 (1999).

¹³Z. Marka, Ph. D. thesis, Vanderbilt University, 2002.

¹⁴B. S. Wherret, J. Opt. Soc. Am. B **1**, 67 (1984).

¹⁵V. K. Adamchuk and V. V. Afanas'ev, Prog. Surf. Sci. **41**, 111 (1992).

¹⁶J. Robertson, J. Vac. Sci. Technol. B **18**, 1785 (2000).

¹⁷R. Williams, Phys. Rev. **140**, A569 (1965).

¹⁸V. V. Afanas'ev, M. Houssa, A. Stesmans, and M. M. Heyns, Appl. Phys. Lett. **78**, 3073 (2001).

¹⁹J. W. Keister, J. E. Rowe, J. J. Kolodziej, H. Niimi, T. E. Madey, and G. Lucovsky, J. Vac. Sci. Technol. B **17**, 1831 (1999).

²⁰S. Miyazaki, H. Nishimura, M. Fukuda, L. Ley, and J. Ristein, Appl. Surf. Sci. **113/114**, 585 (1997).

²¹J. I. Dadap, X. F. Hu, M. H. Anderson, M. C. Downer, J. K. Lowell, and O. A. Aktsipetrov, Phys. Rev. B **53**, R7607 (1996).

²²J. G. Mihaychuk, N. Shamir, and H. M. van Driel, Phys. Rev. B **59**, 2164 (1999).

²³Y. Takemura, J. Ushio, T. Mariuzumi, K. Kubota, and M. Miyao, Mater. Sci. Semicond. Process. **2**, 253 (1999).